

Photoinduce dichroism as a tool for understanding orientational mobility of photoisomerizable dyes in amorphous matrices[☆]

Michel Fischer^a, Ahmad El Osman^b, Pierre-Alexandre Blanche^c, Michel Dumont^{a,*}

^aLPQM, CNRS (UMR 8537), ENS de Cachan, 61 Av du Président Wilson, 94235 Cachan cedex, France

^bLaboratoire Charles Fabry de l'Institut d'Optique, CNRS (UMR 8510), BP 147, 91403 Orsay cedex, France

^cCentre Spatial de Liège, Parc Scientifique du Sart Tilman, Avenue du Pré-Aily, 4031 Angleur-Liège, Belgium

Abstract

In amorphous materials, the excitation of photoisomerizable dye molecules (most often azo dyes) by polarized light induces a more or less permanent anisotropy (dichroism and birefringence). Photoinduced anisotropy (PIA) is the result of the competition of three processes: (1) Angular hole burning (AHB) by polarized light; (2) Angular redistribution (AR) during the photoisomerization, the lifetime of the photo-isomer and the (spontaneous or photoinduced) return to the stable isomeric structure; (3) Thermal diffusion in the ground state. Photoassisted electrical poling (PAEP) and all-optical poling (AOP) proceed from the same mechanisms, but with different symmetries. In order to study optical ordering mechanisms and to characterize materials for photonic applications, a multiple wavelength experimental setup is used for recording the dynamics of the growing and of the relaxation of photoinduced dichroism. Results are interpreted with the help of a simple phenomenological model based on diffusion and pumping rates. Several examples are presented which illustrate the ability of this method for characterizing the orientational behavior of dye molecules. © 2000 Elsevier Science S.A. All rights reserved.

Keywords: Photoinduced anisotropy; Photoisomerization; Material for non linear optics

1. Introduction

Three different optical methods have been developed for ordering dye molecules in polymer films, for nonlinear optics and photonics applications.

- Photoinduced anisotropy (PIA) or Weigert effect: birefringence and dichroism are induced by a polarized resonant light excitation.
- Photoassisted electrical poling (PAEP): optical pumping increases the mobility of molecules, which can be oriented by the field at room temperature [1,2].
- All-optical poling (AOP) is the most recent method: the material is coherently pumped by the fundamental frequency and the second harmonic of a laser beam resonant at 2ω [3–5]. A $\chi^{(2)}$ can be created with non-polar molecules (octupolar molecules) and different macroscopic symmetries can be induced [6].

These three ordering processes are very efficient with photoisomerizable chromophores and the common mechanism is now well understood [7] and described by a math-

ematical model [8,9]. Fig. 1 gives a phenomenological description of photoinduced anisotropy, in the case of Dispersed Red 1 (DR1). In a first step, anisotropic *trans* molecules are selectively excited by a linearly polarized resonant pump beam, with a probability proportional to $\cos^2\theta$, where θ is the angle between the transition dipole moment of the molecule and the light electric field (Fig. 1c). The result is an angular hole burning (AHB) in the population distribution of the *trans* state (Fig. 1d). From electronically excited states, some molecules relax, non radiatively, to the *cis* state, where the angular distribution presents a bump, more or less complementary of the hole in *trans*. *Cis* molecules come back to *trans*, either by spontaneous thermal relaxation or by reverse photoisomerization (Fig. 1b). At each step (*trans* → *cis* isomerization, angular diffusion in *cis*, *cis* → *trans* isomerization, as illustrated by arrows in Fig. 1d), angular redistribution (AR) spreads the distribution of excited molecules, which enhance the shoulders of the hole, when they come back in *trans*. If the thermal diffusion in *trans* is slower than AR mechanisms, the photostationary distribution in *trans* is strongly anisotropic (dotted curve in Fig. 1d). When the pump is switched off, anisotropy decreases according to the angular diffusion rate in *trans*.

AOP differs from PIA, only by the symmetry of hole burning. AHB contains three contributions: two of them are

[☆] With the support of CNRS (projet matériaux).

* Corresponding author. Tel.: +33-1-4740-5559; fax: +33-1-4740-5567.
E-mail address: michel.dumont@lpqm.ens-cachan.fr (M. Dumont).

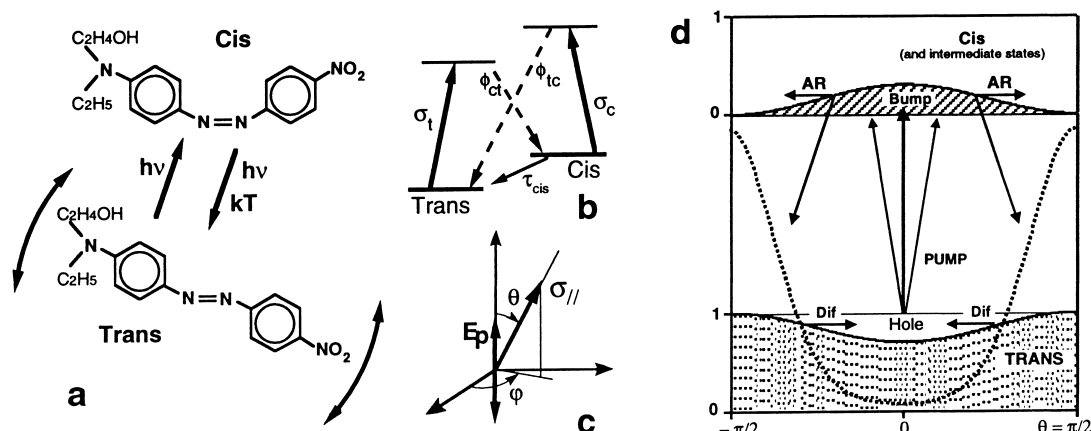


Fig. 1. Mechanisms of PIA induced by photoisomerization: (a) Photoisomerization of DR1; (b) Simplified diagram of levels; (c) Definition of the orientation of the transition dipole moment with respect to the electric field (E_p) of light; (d) Schematic representation of the angular distribution in *trans* and *cis*, in the presence of hole burning, spreading of the distribution by AR (angular diffusion in *cis* and rotation in isomerization processes represented by oblique arrows) and thermal relaxation in *trans* (Dif). The dotted line is the *trans* distribution after several cycles, if Dif is negligible.

centrosymmetric (one-photon absorption at 2ω , proportional to $\cos^2\theta$ and two-photon absorption at ω , proportional to $\cos^4\theta$, if both pumping beams are linearly polarized in the same direction) and the third is non-centrosymmetric, from the interference of ω and 2ω waves ($\propto \cos^3\theta$). With circular or more general elliptical polarizations, the non-centrosymmetric term involves angles θ and φ and can be used for tailoring special tensorial conformations of the non-linear susceptibility [6]. In all cases, AR produces an angular distribution that is complementary of the pumping probability: molecules are accumulated in the less pumped configuration. In PAEP, pumping is centrosymmetric, like in PIA, but AR is non-centrosymmetric since it is driven by a DC electric field. AR is always a random process, but tends toward the thermodynamic equilibrium distribution of the dipoles in the poling electric field. Nevertheless, the final result is not the thermodynamic equilibrium (like in thermal poling) because of the competition between AR and AHB.

In this paper, we show, with the help of several examples, that the analysis of the dynamics of photoinduced dichroism, simultaneously on different wavelengths, is a powerful tool for understanding molecular reorientation. The experimental setup is described on Fig. 2. From the optical densities $OD_{//}$ and OD_{\perp} (analyzer parallel and perpendicular, respectively, to the polarization of the pump beam), two characteristic curves are drawn. The first is the average optical density, $OD_m = S_0$, which depends only on *trans* and *cis* populations, $N_{T,C}$, and on their average absorption cross sections, $\bar{\sigma}_{T,C}(\lambda)$. The second is the anisotropy signal, S_2 , which is a function of order parameters, $\langle P_2 \rangle_{T,C}$ (projection of angular distributions on the Legendre polynomial $P_2(\cos\theta)$)

$$S_{0,\lambda} = OD_m = \frac{1}{3}(OD_{//} + 2OD_{\perp}) = N_T\bar{\sigma}_T(\lambda) + N_C\bar{\sigma}_C(\lambda)$$

$$S_{2,\lambda} = \frac{1}{3}(OD_{//} - OD_{\perp}) \\ = N_T\bar{\sigma}_T(\lambda)a_T(\lambda)\langle P_2 \rangle_T + N_C\bar{\sigma}_C(\lambda)a_C(\lambda)\langle P_2 \rangle_C$$

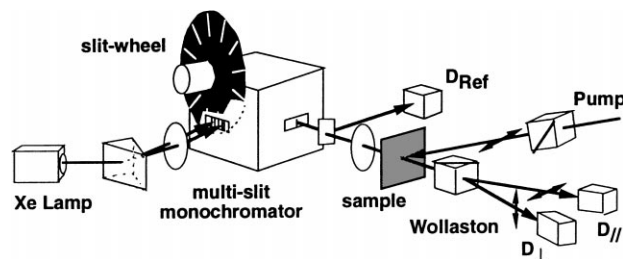


Fig. 2. Multi-wavelength photoinduced dichroism experimental setup. A wheel with narrow slits rotates in front of the six entrance slits of a modified monochromator. The output beam, constituted of a periodic succession of pulses (≈ 2 ms) of different colors, is used as a probe beam and crosses the polarized pump beam on the sample. The probe beam is split into parallel and perpendicular polarization components. A computer, synchronized with the slit wheel, reconstructs the optical densities $OD_{//}$ and OD_{\perp} for each wavelength, as a function of time.

2. Experimental results with different chromophores

2.1. Cx-Cy-DMNPAA

Fig. 3 presents the behavior of two copolymers named Cx-Cy-DMNPAA [10,11] (copolymer of [ω -(*N*-carbazolyl)-alkylmethacrylate] and [4-(11-methacryloylalkoxy)-2,5-dimethylphenyl](4-nitrophenyl) diazene).¹ They differ only by the length of the alkyl spacers which is $x = 6$ (for carbazole radicals) and $y = 11$ (for azo radicals), in the first polymer and $x = 11$ and $y = 6$, in the second one. Samples have been made by hot pressing of polymer powder between two glass plates. The optical density of both samples (Fig. 3D) is too high at the center of the absorption band (≈ 400 nm) and dichroism measurements are possible only on the red wing (450–600 nm).

¹Synthesized by C. Maertens [10], CERM (Prof. R. Jérôme and P. Dubois), Université de Liège, Belgium.

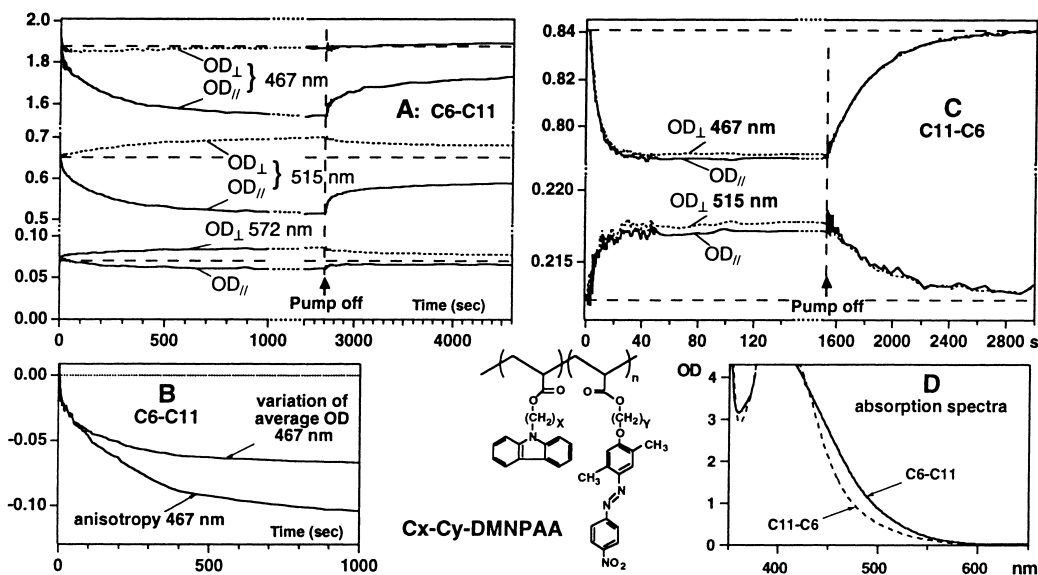


Fig. 3. Formula of Cx-Cy-DMNPAA polymers and experimental results for C6-C11 and C11-C6. The pumping laser beam ($\approx 20 \text{ mW/cm}^2$; $\lambda = 514 \text{ nm}$) is switched on at $t = 0$. Horizontal dashed lines are OD's before pumping. Fig. 3D represents absorption spectra of both samples before pumping.

With C6-C11, the slow widening of the gap between $OD_{//}$ and OD_{\perp} , for the three probe wavelengths represented in Fig. 3A, is characteristic of the existence of angular redistribution induced by the photoisomerization process, but more rigorously convincing is the comparison of S_0 and S_2 , in Fig. 3B. The two curves have been normalized in order to have the same slope during the first second. At the beginning of pumping, population and anisotropy vary in the same way: in this period of time, AHB is preponderant and AR is negligible. But after 1 min, the variation of population begins to saturate, while anisotropy continues to increase. This is the best proof of AR, since it is easy to prove that, in the case of pure AHB without rotation of molecules, anisotropy varies proportionally to population as far as saturation is negligible, i.e. when the *trans* population can be written as $n_T(\theta) = (N_T/2)(1 - \epsilon \cos^2(\theta))$, but saturates faster than population and decreases at high saturation, when almost all molecules are pumped. After the removal of the pump, anisotropy relaxes slowly. In this material, AR is slower than AHB, which means that many photoisomerization cycles are necessary to produce the accumulation of molecules in the perpendicular direction, but this accumulation is possible because the thermal diffusion in *trans* is much slower than AR. The spectral study of the variation of S_0 , shows that there is an isobestic point at 535 nm.

With C11-C6-DMNPAA (Fig. 3C), the behavior is quite different: the variations of the optical density at 467 and 515 nm attest that photoisomerization is efficient and that the isobestic point is between these wavelengths. The photoinduced anisotropy is extremely small and disappears instantaneously when the pump is switched off. This result is not surprising, since the glass transition temperature is $T_g = -20^\circ\text{C}$. Thermal diffusion is very fast as well for both *trans* and *cis*, and erases any anisotropy as soon as it is

created. Another characteristic of the liquid state of this polymer is the perfect exponential variations of the OD's (relaxation rate is 312 s and pumping rate, 6.16 s). In C6-C11, which is a glass ($T_g = +56^\circ\text{C}$), none of the transients are exponential, because of the dispersion of time constants from one molecular site to another. It is interesting to observe a so large difference of T_g from a simple variation of spacer's length. Probably the looser links of carbazole radicals, in C11-C6, allows them to express their well-known plasticizing property.

2.2. Diazo bipyridine in PMMA

This molecule, shown in the inset of Fig. 4 ($2,2'$ [*p*-diazo-*p*-*N,N* dibutyl aniline]bipyridine)² has two $\text{N}=\text{N}$ bonds that can be photoisomerized. Photoisomerization is evidenced, in Fig. 4 (top left) by a decrease of the average optical density spectrum, between 405 and 500 nm and an increase below 405 nm. The isobestic point near 500 nm is not visible on the spectrum, but it is attested by the time variation of OD_m at 554 nm (Fig. 4 top center). The thermal relaxation of photoisomers is rather slow, but almost complete after 14 h. The OD_m spectrum after 1 h is clearly blue shifted, which is confirmed by the difference in the time evolution at 430 and 481 nm (Fig. 4 top right). In a simple two-level model, these variations should be proportional. This spectral shift during optical pumping has been observed with other azo-dyes, such as Disperse Red 1 [13,14].

Anisotropy spectra (Fig. 4 bottom left) and relaxation curves at any wavelength (bottom right) reveal that the photoinduced anisotropy is remarkably stable, for a

² Synthesized by T. Renouard [12], UMR 6509, Université Rennes I (Drs. H. Le Bozec, A. Hilton and O. Maury).

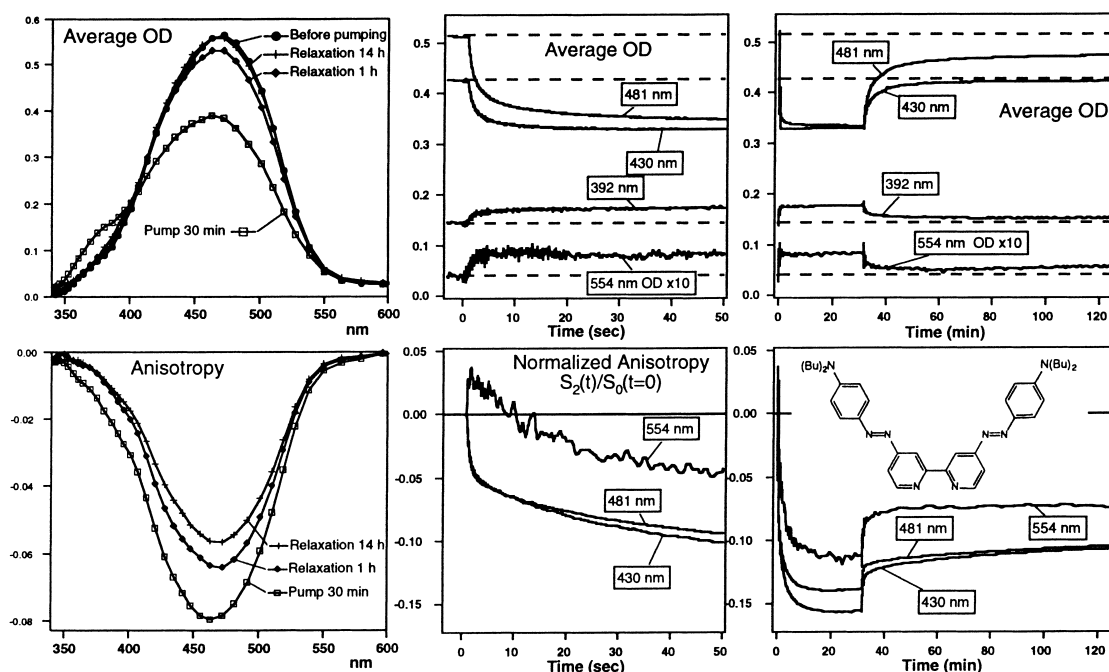


Fig. 4. Experimental results with the diazo bipyridine shown in inset (7.2 wt.% in PMMA). The first row shows the average optical density, S_0 , and the second row the normalized anisotropy: the left graphs represent spectra before pumping, 30 min after the beginning of pumping ($\lambda = 458$ nm, 20 mW/cm²) and 1 and 14 h after the pump is switched off. The central graphs show time variations in the first 50 s and the right graphs, the evolution on 2 h (pump is on at $t = 0$ and off at $t = 30$ min).

guest–host material. It is a proof of a strong AR and a very slow angular diffusion in *trans*, much slower than that of DR1 [13], probably because of the larger molecular size. The predominance of AHB, in the first second and the slow emergence of AR in the following minutes are particularly clear with this molecule. Indeed, when the pump is switched on, anisotropy increases very fast (Fig. 4, bottom center), comparable to the variation of OD_m (top center). Dichroism is negative at 430 and 481 nm (hole in *trans* distribution) and positive at 554 nm and also at 335 and 361 nm (pump in *cis*, Fig. 1d). After 10 s, the anisotropy changes of sign at 554 nm and in the UV and slowly increases with a negative sign, for all wavelengths, as AR progressively accumulates *trans* molecules perpendicular to the pump polarization and partially erases the anisotropy in *cis*: the product of the $\cos^2\theta$ absorption probability by the angular distribution in *trans*, tends to be flat. The probable reverse *cis*–*trans* pumping of molecules, also tends to reverse anisotropy in *cis* (see next paragraph). The fast decay of $\approx 20\%$ of the anisotropy, at the pump extinction, could be due to the partial filling of the hole in *trans* by the relaxation of the remaining bump in *cis*, but this interpretation is a little bit contradictory with previous assertions and the existence of more than two isomers complicates the model.

2.3. Spiropyran-merocyanine photoisomerization

Spiropyrans are well known very efficient photochromes, since they turn from transparent to deep blue when UV light

opens the pyranic ring, which leads to a conjugated merocyanine shape (Fig. 5). This type of molecules can be photo-oriented as well as azo-dyes, but has some interesting properties: the main absorption band of merocyanine is disconnected from that of spiropyran so that it is possible to pump separately the photoisomer, back to the stable isomer. On the other hand, photomerocyanine has a long lifetime (we measured ≈ 17 h in PMMA) and it is easy to study it separately. The S_2 spectrum (Fig. 5, left-top) shows that merocyanine molecules are oriented parallel to the polarization of the UV pump (positive anisotropy). More precisely, from S_2 at short pumping times, we determined an upper limit of 35° , but it is probably much less: this was not expected, since the transition dipole moment of spiropyran is not known and since photoisomerization implies a large change in the structure. According to AHB, S_2 is negative for the UV absorption band of spiropyran [15,16].

With UV pumping alone (first 20 min in left graphs of Fig. 5), one observes that OD_m increases at all wavelengths, but not proportionally to each other, because of a spectral shift. All curves reach a maximum and then decrease (within 20 min the maximum is obtained only with red probes, at 585 and 649 nm). The relative anisotropy (S_2/S_0), which is exactly proportional to the order parameter $\langle P_2 \rangle_M$ of merocyanine molecules, is very large in the first seconds but decreases rapidly to $\approx 15\%$ of its maximum. This behavior is predicted by theory, when the thermal isotropic relaxation of the photoisomer is negligible compared to the anisotropic reverse photoisomerization. Simulations [8,9] are shown in

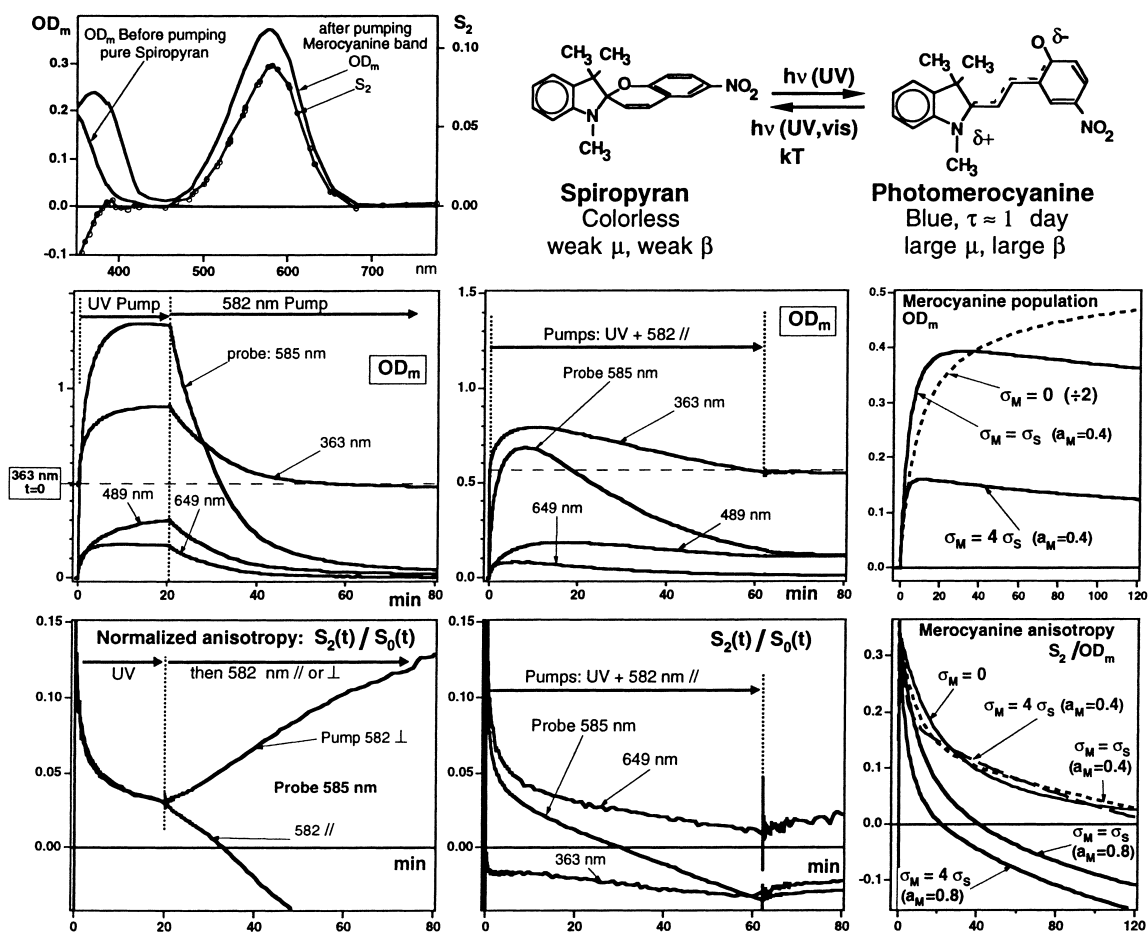


Fig. 5. Spiropyran-merocyanine photoisomerization. The top-left graph shows spectra of merocyanine, (5% in PMMA) obtained with polarized UV pumping (350–400 nm, 1.5 mW/cm², 8 min). The central row shows time variations of OD_m(=S₀) and the bottom row that of the relative anisotropy (25% spiropyran in PMMA). Left hand graphs: 20 min of UV pumping (3 mW/cm²) immediately followed by a 582 nm pumping (12 mW/cm², polarization parallel or perpendicular to that of UV pump). Central column: simultaneous UV and yellow pumping (3 and 30 mW/cm², respectively), during 1 h. Right hand graphs: theoretical simulations [8,9] of S₀(t) and S₂(t)/S₀(t), for different values of the cross section of merocyanine → spiropyran photoisomerization, σ_M and of the merocyanine molecules anisotropy a_M.

the right graphs of Fig. 5, as a function of the cross section of merocyanine → spiropyran photoisomerization, σ_M (more precisely its ratio to the direct isomerization cross section σ_S, including quantum yield factors) and of merocyanine anisotropy a_M = [(σ - σ_⊥)/(σ + 2σ_⊥)]. It appears that a large anisotropic back pumping produces a maximum in OD_m and a change of sign of S₂. With the simple model of AHB of Fig. 1, this means that first excited molecules present a well confined bump in their angular distribution, but after some time, AR broadens it and a strong anisotropic back pumping reduces the bump or even digs a hole in the excited state.

In order to prove this interpretation, we took advantage of the possibility to pump merocyanine alone, with yellow light. In the first experiment (left column in Fig. 5) we applied a 582 nm pump just after UV pumping. As expected, the yellow pump destroys the merocyanine total population (OD_M). The anisotropy of merocyanine molecules is confirmed by the sign of the variations of anisotropy when the polarization of the second pump is parallel or perpendicular to that of the first one. In the second experiment (central

column in Fig. 5), UV and yellow pumps are applied simultaneously with parallel polarizations. This is a means to reinforce the back optical pumping of the UV excitation. We clearly see an earlier maximum in OD_m, followed by a faster decrease and a change of sign of the anisotropy at the center of the absorption band of merocyanine (585 nm).

2.4. Two other molecules

Azobenzen is known for having distinct absorption bands in *trans* (UV) and in *cis* (≈440 nm) and for the absence of thermal *cis* → *trans* relaxation, at room temperature. Fig. 6 (left graph) confirms these properties in a PMMA matrix. Optical density decreases strongly at 335 nm and increases at 450 nm, under the action of a moderate UV pump. When the pump is switched off, the relaxation of *cis* is negligible but a new pumping at 458 nm restores almost immediately the *trans* shape. The photostationary state is modified by a simultaneous illumination with both pumps. The dichroism is always rather small and relaxes by 70% in 10 min, in dark.

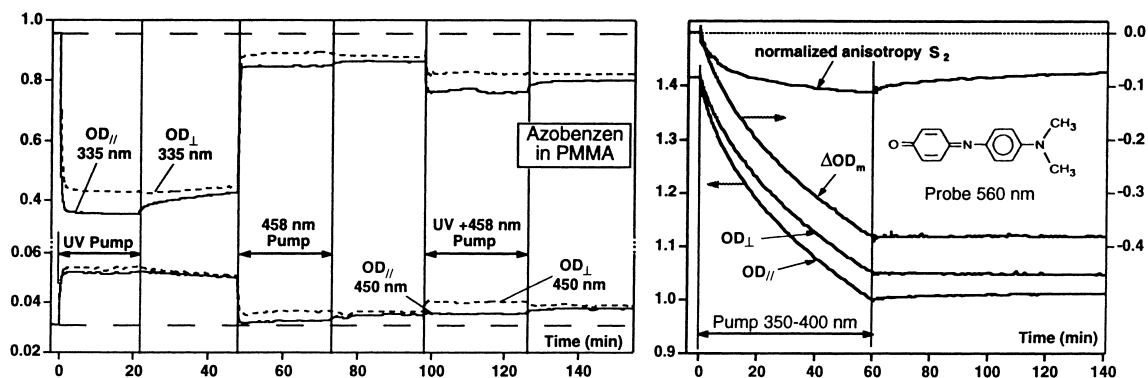


Fig. 6. Left: azobenzene in PMMA (12.5 wt.%). $OD_{//}$ and OD_{\perp} at 335 nm (*trans* band) and 450 nm (*cis*) with pumping at 365 nm (few mW/cm^2) and/or 458 nm ($75 mW/cm^2$). Right: Indoaniline in PMMA (9%). OD and OD_{\perp} near the center of the absorption band (585 nm). ΔOD_m and S_2 have been normalized in order to have the same slope at $t = 0$; the faster saturation of S_2 is characteristic of pure hole burning (here, bleaching).

AR is not very efficient probably because of the absence of thermal relaxation and of back pumping of *cis* by UV, when this pump is alone: the rate of back and forth isomerizations is too low. Relatively, the anisotropy is slightly better with both pumps, but it should be interesting to equilibrate the pumps better than in Fig. 6 and to use crossed polarizations.

Indoaniline has been chosen because it has no photoisomer and it does not fluoresce (the energy of absorbed photons is dissipated in molecular vibrations, like in DR1). Fig. 6 (right graph) shows that $OD_{//}$ and OD_{\perp} are both strongly reduced by the UV pumping. The anisotropy signal, S_2 , has been normalized in such a manner that it has the same slope as the variation of OD_m , at $t = 0$. S_2 saturates much faster than ΔOD_m : it is characteristic of angular hole burning, without angular redistribution. At the removal of the pump, S_2 slightly relaxes, but OD_m is perfectly constant. The behavior of this non-photoisomerizable molecule can be completely explained by an angularly selective photo-degradation. 458 nm pumping produces the same effect if the power is high ($\approx 400 mW/cm^2$).

3. Conclusion

With the help of some examples exhibiting different behaviors, we have shown that a careful study of photo-induced dichroism, performed simultaneously with several probe wavelengths, provides a great deal of information on the photo-orientation properties of dye molecules in amorphous matrices. It is possible to analyze, in each case, the competition between angular hole burning, angular redistribution and angular thermal diffusion. A sensitive test of the existence of AR is the comparison of the dynamics of photo-induced variations of population and of anisotropy. If anisotropy continues to increase when the population saturates, AR is efficient and the material should be suitable for photoassisted electrical poling and all-optical poling. Up to

now, photoisomerization appears to be the necessary mechanism for inducing AR, but efficient back thermally or optically induced isomerization is an important factor, since molecules need a large number of back and forth isomerizations to be reoriented. The larger the stability of the final order, the larger is the needed number of cycles, since both depends on the size of the chromophore, on the strength of its links to the polymer chain (see ref [12] for grafted chromophores) and on the glass transition temperature.

References

- [1] Z. Sekkat, M. Dumont, Appl. Phys. B 54 (1992) 486–489.
- [2] Z. Sekkat, M. Dumont, Nonlinear Optics 2 (1992) 359–362.
- [3] F. Charra, F. Kajzar, J.M. Nunzi, P. Raimond, E. Idiart, Optics Lett. 18 (1993) 941.
- [4] C. Fiorini, F. Charra, J.M. Nunzi, P. Raimond, Nonlinear Optics 9 (1995) 339.
- [5] J.M. Nunzi, F. Charra, C. Fiorini, J. Zyss, Chem. Phys. Lett. 219 (1994) 349.
- [6] S. Brasselet, J. Zyss, J. Opt. Soc. Am. B 15 (1998) 257–288.
- [7] M. Dumont, G. Froc, S. Hosotte, Nonlinear Optics 9 (1995) 327–338.
- [8] M. Dumont, in: F. Kajzar (Ed.), Photoactive Organic Molecules, Science and Applications, Nato ASI Series, Vol. 9, Kluwer Academic Publishers, Dordrecht, 1996, pp. 501–511.
- [9] M. Dumont, Chem. Phys. 1999, in press.
- [10] C. Maertens, Synthesis and characterization of new macromolecular materials for non linear optics, Thesis, Université de Liège, Belgium, 1998.
- [11] P.A. Blanche, P. Lemaire, C. Maertens, P. Dudois, R. Jérôme, SPIE 3417 (1998) 131.
- [12] T. Renouard, Synthèse, caractérisation et propriété de non-linéarité optique de nouveaux complexes octupolaire à ligands bipyridyle, Thesis, Université de Rennes I, France, 1998.
- [13] A. El Osman, M. Dumont, Proc. SPIE 3417 (1998) 36.
- [14] A. El Osman, M. Dumont, Polym. Preprints 39 (1998) 300.
- [15] A. El Osman, M. Dumont, Polym. Preprints 39 (1998) 1036.
- [16] A. El Osman, Etude des mécanismes d'orientation photoinduite de molécules de colorants dans des films de polymère, Thesis, Université Paris XI, Orsay, France, 1998.